Clays and Clay Minerals, Vol. 40, No. 5, 501–514, 1992.

MICROSTRUCTURES, MIXED LAYERING, AND POLYMORPHISM OF CHLORITE AND RETROGRADE BERTHIERINE IN THE KIDD CREEK MASSIVE SULFIDE DEPOSIT, ONTARIO[1]

WEI-TEH JIANG,[2] DONALD R. PEACOR,[2] AND JOHN F. SLACK[3]

[2] Department of Geological Sciences
The University of Michigan, Ann Arbor, Michigan 48109

[3] U. S. Geological Survey, National Center, M.S. 954, Reston, Virginia 22092

Abstract—Transmission electron microscopy (TEM) was utilized to determine the origins of berthierine and chlorite in the core of the footwall alteration zone of the Kidd Creek massive sulfide deposit, Ontario. TEM images show lamellar intergrowths of packets of berthierine, mixed-layer chlorite/berthierine, Fe-Mg chlorite, and relatively Fe-rich chlorite that contain dislocations, stacking faults, kink bands, and gliding along (001). Interstratification of packets of berthierine and chlorite with one to several tens of layers commonly is associated with terminations of a layer of chlorite by two layers of berthierine. Layers in adjacent domains of berthierine and chlorite are continuous across interfaces that transect their common {001} planes. High-strain zones that cut across cleavage planes, consisting of distorted layers and lens-shaped pores, are associated with stacking faults and gliding along cleavage planes in chlorite crystals. Similar features separate interstratified chlorite/berthierine of different structures and textures, implying development of such composite grains after deformation of chlorite. Electron diffraction patterns show that the chlorite is an ordered one- or two-layer polytype or a one-layer polytype with semi-random stacking, and that the berthierine is a one-layer polytype with semi-random stacking epitaxially intergrown with chlorite.

Coexisting chlorite and berthierine have nearly identical ranges of compositions, containing Si ≅ 5, Al ≅ 6, and Fe ≅ 6.5–8.5 pfu, and minor, variable Mg and Mn contents, in formulae normalized on the basis of 20 total cations. This implies polymorphism among Fe,Al-rich members of the serpentine and chlorite groups. In one of the samples, berthierine and mixed-layer chlorite/berthierine coexist with chlorite having two compositional ranges, including Fe-rich chlorite with a relatively wide range of Fe-Mg contents, and a dominant Fe-Mg chlorite. In another sample, compositionally homogeneous Fe-rich chlorite is associated with berthierine and mixed-layer chlorite/berthierine; Fe-Mg chlorite was not detected.

The microstructural relations and the presence of coexisting polymorphs, complex mixed layering, heterogeneous polytypism, and wide ranges of mineral compositions are consistent with replacement of chlorite by berthierine under non-equilibrium retrograde conditions, in contrast to the generally assumed prograde origin for other berthierine occurrences.

Key Words—Berthierine, Chlorite, Massive sulfide deposit, Microstructures, Mixed layering, Polymorphism, Polytypism, Transmission electron microscopy.

INTRODUCTION

Berthierine is a common Fe-rich aluminous phyllosilicate in iron formations (Bhattacharyya, 1983; Chamley, 1989; Young, 1989). It is a 1:1 member of the serpentine group with 7-Å periodicity (Bailey, 1984, 1988a), but is unique in having high Fe and Al contents. Even though simplified formulae of the serpentine and chlorite groups [$M_6T_4O_{10}(OH)_8$] imply a shared polymorphic relation, the complex compositions of chlorite do not overlap those of the more restricted compositions of 1:1 phyllosilicates such as berthierine. Ahn and Peacor (1985) reported apparent overlap in the compositions of intergrown berthierine and chlorite in Gulf Coast sediments; however, the compositions of coexisting phases were only determined indirectly. Based on literature surveys, Curtis *et al.* (1985), Hughes (1989), and Jahren and Aagaard (1989) also made comparisons of the compositions of berthierine and chlorite, but not in the context of polymorphic relations. The principal difficulty in documenting such a relation lies in access to well-characterized, pure berthierine. The occurrence of berthierine and Fe-rich chlorite in the Kidd Creek massive sulfide deposit, Ontario, recently reported by Slack *et al.* (1992), offers an exceptional opportunity to investigate the possible existence of polymorphism among Fe,Al-rich members of the serpentine and chlorite groups; these phases in this locality are relatively coarse grained and yield reliable analyses, especially by high-resolution analytical electron microscopy (AEM).

The formation of most berthierine in iron formations has been inferred to involve diagenetic and hydrothermal alteration of pre-existing phases, mainly ka-

[1] Contribution No. 493 from the Mineralogical Laboratory, Department of Geological Sciences, The University of Michigan, Ann Arbor, Michigan 48109.

olinite, or direct precipitation from fluids and gels (e.g., Bhattacharyya, 1983; Young, 1989). Powder X-ray diffraction and chemical analytical data have led to the identification of berthierine in only a small number of shallow marine sediments and unmetamorphosed clastic sedimentary rocks (Velde *et al.*, 1974; Frey, 1970, 1978; Iijima and Matsumoto, 1982; Curtis *et al.*, 1985; Taylor, 1990; Walker and Thompson, 1990). However, transmission electron microscopic (TEM) observations of clastic sediments have shown that berthierine typically is admixed with diagenetic chlorite at very fine scales (e.g., Lee and Peacor, 1983; Ahn and Peacor, 1985; Amouric *et al.*, 1988; Jahren and Aagaard, 1989; Jiang *et al.*, 1990). Powder X-ray diffraction patterns of bulk samples or clay separates of such sediments commonly lack indications of berthierine or mixed-layer chlorite/berthierine. Identification by powder X-ray diffraction of small amounts of berthierine in the presence of chlorite is hampered by the overlap of 00*l* reflections with those of chlorite. These relations thus suggest that berthierine may be a common phase in low-temperature environments and that it frequently is undetected in routine mineralogical studies.

Berthierine is generally considered a metastable precursor of chlorite in diagenetic environments (e.g., Kisch, 1983; Ahn and Peacor, 1985; Weaver, 1989; Walker and Thompson, 1990). On the other hand, berthierine has also been shown to be a retrograde alteration product of chloritoid or its retrograde successors (mainly chlorite) in metapelites of polymetamorphic origin (Banfield *et al.*, 1989). The onset of the transition from berthierine to chlorite during prograde metamorphism is believed to occur at temperatures of 70°–200°C (Velde *et al.*, 1974; Iijima and Matsumoto, 1982; Jahren and Aagaard, 1989; Walker and Thompson, 1990). Relations between berthierine and chlorite in a given occurrence therefore may have important implications for the thermal history of an area.

Based on the presence of large prismatic berthierine grains, coexistence of mixed-layer chlorite/berthierine with chlorite, and equilibrium textures between subhedral berthierine and muscovite, Slack *et al.* (1992) suggested that pre-metamorphic hydrothermal growth was the principal mechanism of formation for the Kidd Creek berthierine. They proposed that berthierine formed by hydrothermal replacement of aluminous phases such as muscovite or chlorite. Because of the additional presence of composite grains consisting of stacks of berthierine and deformed chlorite packets, and rimming of such composite grains by berthierine, Slack *et al.* (1992) also suggested that retrograde metamorphic or syn- to post-metamorphic hydrothermal replacement of chlorite by berthierine was a formation mechanism for some of the Kidd Creek berthierine. Additional TEM work on the same Kidd Creek samples subsequently has revealed striking and unusually complex intergrowths of berthierine and chlorite, leading to further inferences concerning formation sequences and polymorphic relations between berthierine and chlorite that are reported here.

GEOLOGIC SETTING AND EXPERIMENTAL TECHNIQUES

Kidd Creek massive sulfide deposit

The Kidd Creek volcanogenic massive sulfide deposit is located approximately 27 km north of Timmins, Ontario, in the western part of the Abitibi greenstone belt within a sequence of metamorphosed felsic and mafic volcanic rocks of Archean age (Walker *et al.*, 1975; Brisbin *et al.*, 1990). The Kidd Creek Cu-Pb-Zn-Ag ores are hosted by rhyolitic volcaniclastics intercalated with discontinuous stratiform lenses of carbonaceous argillite and chert, and are closely associated with massive intrusive rhyolite. Intermediate to mafic dikes are also present locally. The sulfide deposit is believed to have formed synchronously with the volcaniclastic and sedimentary host rocks during an episode of subaqueous rhyolitic volcanism (Walker *et al.*, 1975).

The Kidd Creek deposit consists of two ore bodies separated by a major shear zone. The north ore body, from which the studied samples were collected, has a large chalcopyrite stringer zone and associated carbonaceous argillite and massive to brecciated rhyolites (Walker *et al.*, 1975). Geology and whole-rock geochemistry of the footwall alteration zone are described by Coad (1985). Post-ore polymetamorphic and deformational history of the area is evidenced by mineral assemblages of the wall rocks and by various deformational features (Walker *et al.*, 1975; Nunes and Pyke, 1981; Percival and Krogh, 1983; Brisbin *et al.*, 1990; Barrie and Davis, 1990). The maximum metamorphic grade is believed to have corresponded with the lower to middle greenschist facies. A subsequent metasomatic event affecting the mine area was also inferred by Maas *et al.* (1986).

Previous mineralogical studies

Microprobe analyses of Kidd Creek chlorite show compositions ranging from those of ripidolite to daphnite, with constant Si and Al contents (Si ≅ 5 and Al ≅ 6 normalized to $O_{20}(OH)_{16}$; Slack and Coad, 1989, Table 2; Slack *et al.*, 1992, Table 2) and with higher Fe contents and larger variations in Fe/(Fe+Mg) in samples from the core of the stringer zone near massive rhyolite sills. Relatively homogeneous, Fe-Mg chlorite was believed to have formed first in an early hydrothermal event that caused sealing of the footwall alteration zone against seawater infiltration. In this model, chlorite was inferred to have been partially replaced by Fe-rich chlorite due to the interaction of Fe-rich endmember hydrothermal fluids related to intrusion of the rhyolite sills (Slack and Coad, 1989). Some of

this Fe-rich chlorite recently has been identified as berthierine by Slack *et al.* (1992) using powder X-ray diffraction and TEM techniques. They suggested that the berthierine formed by hydrothermal and metamorphic alteration of early hydrothermal muscovite or chlorite, based on the occurrence of large euhedral crystals of berthierine intergrown with muscovite and on the occurrence of deformed chlorite grains interlayered with and rimmed by berthierine.

Samples

The data presented here were obtained on samples KC-2505 and KC-813 from the core of the footwall alteration zone where chlorite is Fe-rich and locally shows a wide range of Fe/(Fe+Mg) ratios. Detailed geologic maps and sample localities can be found in Slack and Coad (1989). Powder X-ray diffraction patterns of clay separates of the samples were described by Slack *et al.* (1992). Sample KC-2505 consists of massive chalcopyrite, subordinate quartz, albite, tourmaline, carbonate, arsenopyrite, pyrite, and muscovite-chlorite-berthierine intergrowths that locally define a crenulated foliation. Some of the phyllosilicate grains are bent and kinked (see Slack *et al.*, 1992). Microprobe analyses of chlorite in the sample show compositions ranging from ripidolite to daphnite (Slack and Coad, 1989).

Sample KC-813 contains pyrite, tourmaline, sphalerite, chlorite, quartz, and minor REE-bearing carbonates (bastnaesite group), galena, muscovite, and berthierine. Muscovite commonly occurs as coarse-grained subhedral grains crosscut and/or embayed by anhedral to subhedral berthierine. The phyllosilicate grains are relatively equant and have cleavage planes and elongated outlines parallel or subparallel to a poorly defined foliation. No apparent deformational features were observed within individual phyllosilicate grains by scanning electron microscopy. As shown by the TEM results described below, however, the berthierine grains are actually composed of mixed-layer chlorite/berthierine and chlorite in addition to berthierine, and display a variety of strain features. It was difficult to distinguish chlorite from berthierine in this sample with back-scattered electron imaging because of compositional similarities. Samples KC-2505 and KC-813 both show irregular embayment textures between sulfides and phyllosilicates, and in some cases between phyllosilicate grains, probably reflecting the gliding of phyllosilicates on {001} and/or crystal boundaries during polymetamorphic/deformational events.

Transmission electron microscopy

Ion-milled specimens were characterized by electron diffraction, conventional and lattice-fringe imaging, and analytical electron microscopy. Specimen preparation and instrumental settings were detailed in Jiang and Peacor (1991) and Slack *et al.* (1992). A selected area aperture 10 μm in diameter was utilized to produce the electron diffraction patterns. The aperture covers a specimen area ~0.27 μm in diameter, but areas at thin edges that were much smaller than that were frequently selected for electron diffraction. The data shown below were all carefully verified by moving specimens around the aperture to define areas of interest so that direct correspondence between images and electron diffraction patterns were obtained.

Identification of chlorite and berthierine

Because chlorite and berthierine may have similar compositions (e.g., Jahren and Aagaard, 1989; Velde, 1985, 1989; Slack *et al.*, 1992), EDS analyses may not result in unambiguous identification; identification, therefore, was principally made through lattice-fringe images and electron diffraction patterns.

Lattice fringes of chlorite commonly show 14-Å periodicity, with or without alternating 9- and 5-Å fringes corresponding to talc-like 2:1 layers and brucite-like sheets, respectively (e.g., Veblen, 1983; Ferrow *et al.*, 1990). However, chlorite may display two 7-Å fringes resembling serpentine-like layers under certain conditions (e.g., Amouric *et al.*, 1988; Guthrie and Veblen, 1990). Transitions from 7- to 14-Å phases may be inferred only with difficulty, especially in areas where thickness of thin edges and/or orientation of crystals change rapidly, giving rise to changes in images that may not be due to changes in structure. Changes in thickness of thin edges are generally expressed by banded contrast over a relatively large area compared to the size of a unit cell (Edington, 1975), and are unlikely to be restricted to distances corresponding to the thickness of one or a few layers. In addition, abrupt changes of crystal orientation may occur in highly strained crystals, giving rise to changes between 7- and 14-Å periodicity in images that are not due to structural changes. Such strained regions can generally be recognized by their strain contrast. Through-focus imaging then allows unambiguous identification of 7-Å layers.

Electron diffraction may further confirm identification if areas of interest can be completely isolated by the diffraction aperture. Reflections of 00*l* rows of berthierine and chlorite have periodicities of 7 and 14 Å, respectively. Mixed-layer chlorite/berthierine gives weak, diffuse odd-order reflections, strong, sharp even-order 00*l* reflections, and streaking along c* (e.g., Ahn and Peacor, 1985; Slack *et al.*, 1992). In practice, a combination of electron diffraction and through-focus imaging techniques is more efficient in identifying clay minerals than image simulation for one-dimensional lattice fringes because of restrictions due to variations in crystal thickness and orientation (Guthrie and Veblen, 1990) and lack of recognizable one-dimensional features under certain focus conditions. Unless otherwise stated, interpretations of images presented in

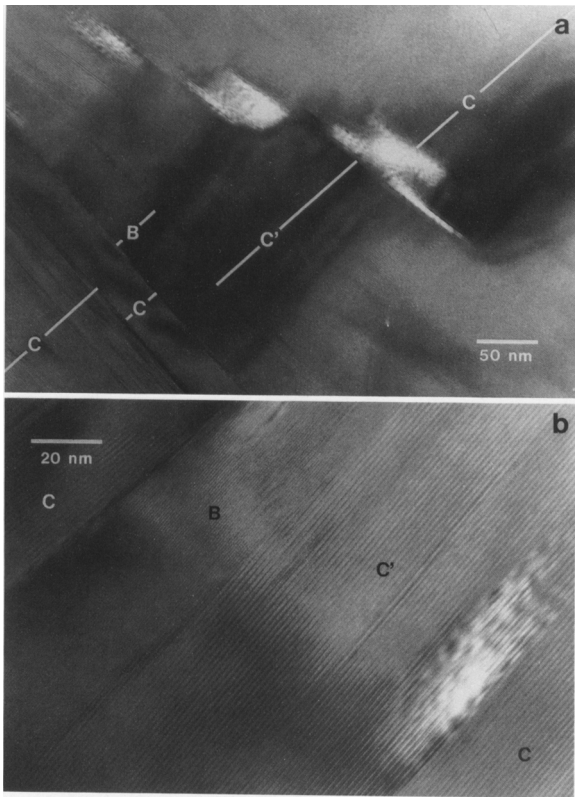

Figure 1. (a) Transmission electron micrograph of a lamellar intergrowth of berthierine and chlorite in sample KC-2505. The chlorite has two compositions; one is more Fe-rich than the other. B = berthierine, C = Fe-Mg chlorite, C′ = relatively Fe-rich chlorite. Banded contrast subnormal to the chlorite cleavage represents kinking in (001). (b) Lattice-fringe image of part of (a) showing detailed textures at crystal boundaries and defects in chlorite crystals.

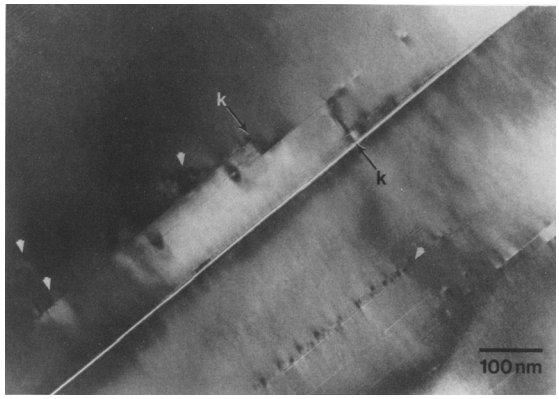

Figure 2. Transmission electron micrograph of two chlorite crystals in sample KC-813. The chlorite crystals have a number of dislocations (alternating bright and dark contrast indicated by white arrows) and stacking faults (linear features with different contrast). A subgrain boundary in the center of the figure is defined by stacking faults, dislocations, and kink bands (indicated by black arrows).

this paper were determined through the above-described criteria and procedures.

TEM OBSERVATIONS

TEM data for samples KC-2505 and KC-813 are described separately, as the samples differ both in texture and composition. Some of the data for sample KC-2505 given by Slack *et al.* (1992) are incorporated here for completeness.

Sample KC-2505

This sample contains four principal types of phyllosilicates, including muscovite, berthierine, mixed-layer chlorite/berthierine, and chlorite having a wide range of Fe/Mg ratios. The chlorite is of two types: one has an intermediate Fe/Mg ratio (hereafter called Fe-Mg chlorite) with a rather restricted compositional range (the dominant type), and the other is a more Fe-rich chlorite of relatively variable composition. Lamellar intergrowths of parallel or subparallel packets of phyllosilicates occur in a matrix of sulfides in this sample. Within those lamellar intergrowths, crystals commonly are bent (principally muscovite) or kinked (principally Fe-Mg chlorite).

Deformed composite grains of lamellar intergrowths of packets of berthierine and chlorite with a berthierine rim have been described by Slack *et al.* (1992). Mixed-layer chlorite/berthierine in such grains is intergrown with Fe-Mg chlorite or Fe-rich chlorite, the latter having a wide range of Fe/(Fe+Mg) ratios. Figure 1 shows an example of lamellar intergrowths in which packets of berthierine and Fe-rich chlorite occur within Fe-Mg chlorite (also see Figure 3 in Slack *et al.*, 1992). Berthierine 001 fringes are parallel to and appear continuous with fringes in adjacent Fe-rich chlorite, although the crystal boundary is oblique to (001) of the related crystals. Such a crystal contact is not a typical, low-angle boundary because layers of contiguous phases are parallel and apparently continuous, without obvious dislocations associated with layer terminations. This kind of crystal boundary has been observed to form during the low-grade contact metamorphic reaction of antigorite to olivine and talc, in which the surfaces [oblique to (001)] of antigorite crystals served as nucleation sites for overgrowths of talc (Worden *et al.*, 1991). The lack of strain contrast at the contact indicates that there is little or no lattice misfit, reflecting minimal differences in thickness and structure of two layers of berthierine and one layer of chlorite. The most likely origin of this texture is through overgrowth of the berthierine by the Fe-rich chlorite, or vice versa. Figure 1a also illustrates an intergrowth relation between Fe-Mg chlorite and Fe-rich chlorite, in which bands of strong strain contrast (parallel to the labeled white lines) are oriented normal to (001) and the layers are parallel within both phases, reflecting changes of crystal orientations within (001). Such orientational

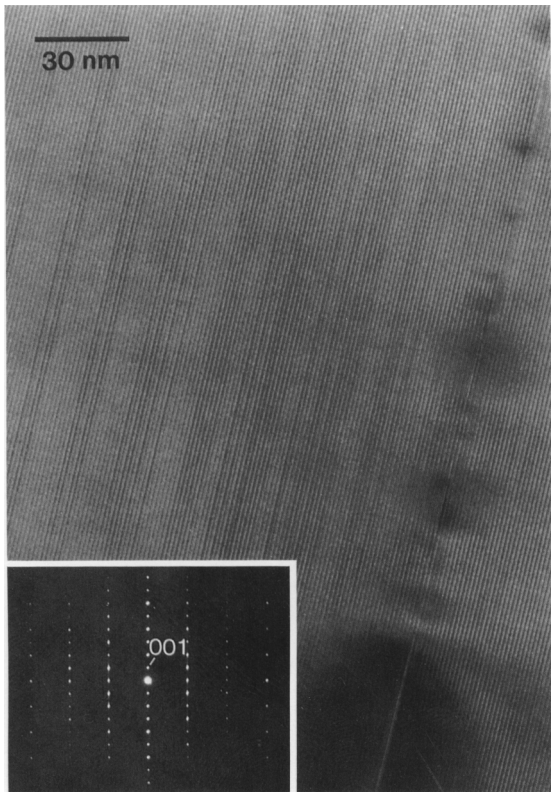

Figure 3. Lattice-fringe image of chlorite showing layers with different contrast due to stacking faults. The corresponding electron diffraction pattern (inset) displays weak streaks along c* in 02*l* and 04*l* but not in $k = 3n$ reflection rows, consistent with the presence of stacking faults in a regular one-layer polytype ($\alpha = 90°$, $\beta \cong 97°$).

changes may be due to bending or kinking of crystals in the cleavage plane. Apparent pores separating the Fe-Mg chlorite and Fe-rich chlorite crystals may have been weakened areas with a high defect density that were thinned preferentially by the ion-milling process.

Sample KC-813

Sample KC-813 contains relatively equant grains of phyllosilicates constituting an assemblage identical to that in sample KC-2505, except that all of the chlorite in sample KC-813 is uniformly Fe-rich and homogeneous in composition. Each phyllosilicate grain is a thick composite stack of packets of berthierine, mixed-layer chlorite/berthierine, and chlorite that is bordered by a cleavage plane or by a high-strain zone cutting across the cleavage. Or the grain simply consists of several packets of muscovite. Chlorite exhibits a variety of defects including kink bands, stacking faults, and dislocations. Figure 2 shows a number of defects in two adjacent chlorite packets. Several dislocations (marked by white arrows) in the (001) plane are clearly present, as expressed by alternating bright and dark contrast. Such dislocations commonly are associated

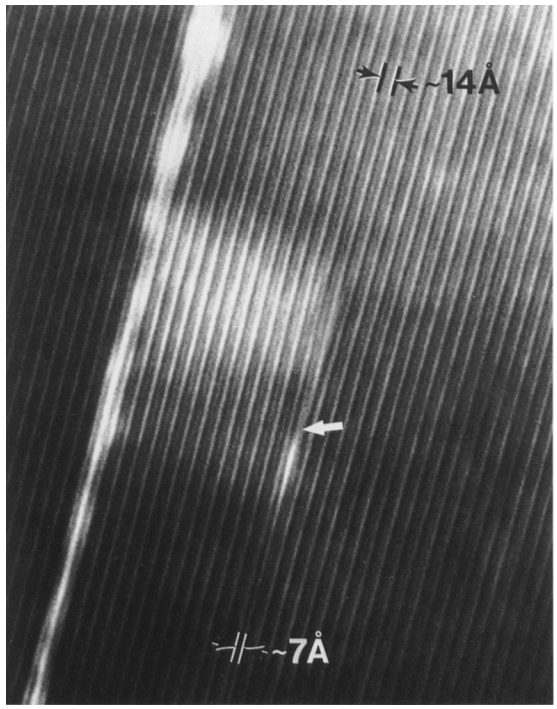

Figure 4. Lattice-fringe image of a relatively unaltered chlorite crystal in sample KC-813. A layer transition from chlorite (wide fringes) to berthierine (narrow fringes) is associated with a partial dislocation at the lower middle (highlighted with a white arrow).

with linear features (Figures 2 and 3) that have different contrast parallel to (001), probably reflecting stacking faults due to local differences of either (1) ±120° rotations of the upper tetrahedral sheet relative to the lower tetrahedral sheet about c* in each 2:1 layer; or (2) $\pm b/3$ shifts between unit layers, because only 0*kl* ($k \neq 3n$) reflection rows with streaking and $k = 3n$ reflection rows without streaking are observed in electron diffraction patterns (Figure 3). These features are likely caused by gliding along (001). Subgrain boundaries that are defined by kink bands (highlighted with black arrows) normal to the cleavage and stacking faults and dislocations parallel to (001) are present in the middle of Figure 2. These textures are similar to the deformation features of chlorite observed by Bons (1988), although we did not observe microfolding. Single berthierine layers are observed to be associated with partial dislocations in chlorite crystals, as illustrated in Figure 4.

Figure 5 shows a zone with significant distortion of layers that cuts across 001 fringes of chlorite. Chlorite layers in the high-strain zone apparently are distorted with strain components parallel and normal to the cleavage. Such a high-strain zone is somewhat similar to the microshear zone in biotite from the Santa Rosa mylonite zone described by Goodwin and Wenk (1990). One side of a high-strain zone commonly has more

Figure 5. Transmission electron micrograph of a chlorite grain in sample KC-813, illustrating a high-strain zone with abundant layer distortions cutting across the cleavage. Stacking faults (linear contrast features) are abundant on both sides of the high-strain zone.

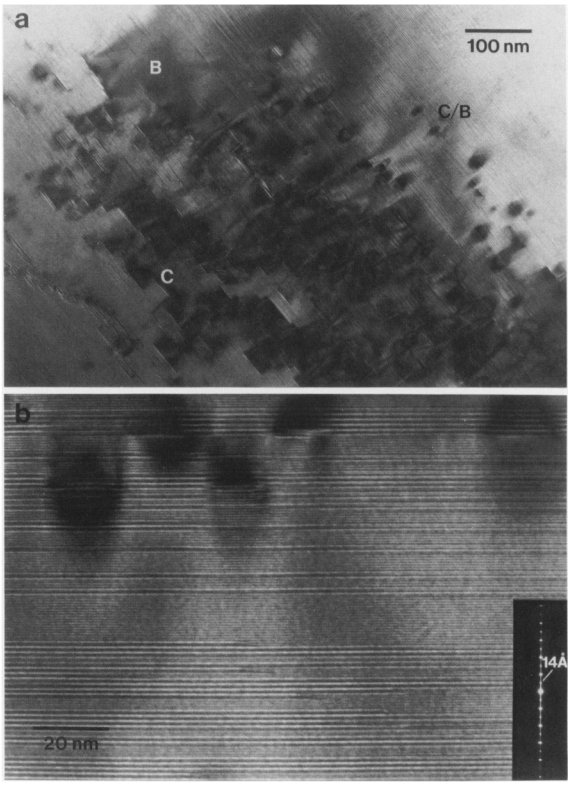

Figure 6. (a) Transmission electron micrograph of a composite chlorite-berthierine grain in sample KC-813 showing a high-strain zone that separates chlorite (C) from berthierine (B) and mixed-layer chlorite/berthierine (C/B). Chlorite layers are highly distorted in the high-strain zone. (b) Lattice-fringe image of the mixed-layer region in (a). Note interstratification of packets of chlorite (wide fringes) and berthierine (narrow fringes) of various thicknesses. Conversions of one layer of chlorite to two layers of berthierine in adjacent layers are common. Areas of high strain contrast are present locally, e.g., upper half of (b), probably due to lateral misfit between chlorite and berthierine layers. Inset shows an electron diffraction pattern of the mixed-layer region.

strain features than does the other side, but no chemical difference is observed. Association of such a high-strain zone with stacking faults is common. High-strain zones also occur among berthierine, mixed-layer chlorite/berthierine, and chlorite, generally in association with lens-shaped pores and abundant kink bands (Figures 6 and 7). Stacking faults are only observed in some of the chlorite crystals in such regions.

Figure 6a shows a broad, high-strain zone separating relatively unstrained chlorite and berthierine plus mixed-layer chlorite/berthierine. The high-strain zone consists largely of distorted chlorite layers showing marked variations in contrast. Kink bands, stacking faults, and local bending of layers are the principal types of defects. The chlorite is a one-layer polytype with semi-random stacking as indicated by electron diffraction (not shown). Berthierine and mixed-layer chlorite/berthierine are relatively unstrained compared to chlorite.

Random interstratification of berthierine and chlorite layers is particularly striking in the Kidd Creek samples because of its complexity and the high concentrations of along-layer transition boundaries. Figure 6b is a lattice-fringe image of the mixed-layer region shown at lower power in Figure 6a; it shows interstratification of packets of berthierine and chlorite. The corresponding electron diffraction pattern shows prominent streaking, weak and diffuse odd-order 00*l* reflections, and strong and sharp even-order 00*l* reflections, corresponding to chlorite with randomly interstratified berthierine. The sharpness of all reflections, however, is unusual compared to typical random mixed-layer chlorite/berthierine in which the number of consecutive layers of a phase is smaller (e.g., Ahn and Peacor, 1985).

Figure 6b also shows abundant terminations of one layer of chlorite by two layers of berthierine with little or no strain contrast. Change of focus conditions did not change the appearance of the 7 Å regions. Distortion of layers associated with strain contrast is present locally but is not related to the change of layer periodicities. It is apparent that such layer transitions occur in

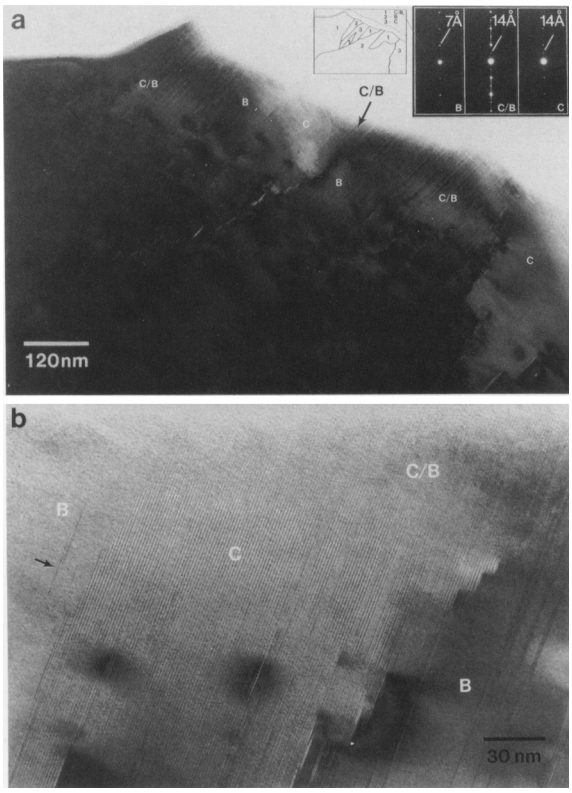

Figure 7. (a) Transmission electron micrograph of a composite chlorite-berthierine grain in sample KC-813. The layers of berthierine (B), chlorite (C), and mixed-layer chlorite/berthierine (C/B) are parallel, but phase boundaries are subparallel to the layers. Insets show electron diffraction patterns characteristic of berthierine, mixed-layer chlorite/berthierine, and chlorite, and a schematic diagram (numbers 1 = C/B, 2 = B, and 3 = C) of the imaged area. (b) Lattice-fringe image of the central part (marked by a black arrow) of (a) showing detailed textures across a high-strain zone consisting of several kink bands and lens-shaped pores that separates packets of berthierine and mixed-layer chlorite/berthierine. Islands and thin packets of 14-Å layers are present within the berthierine crystals.

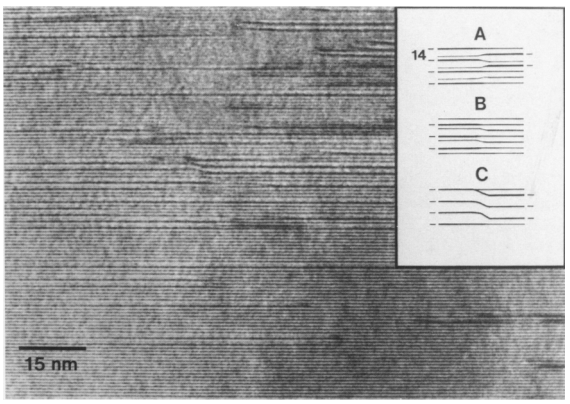

Figure 8. Lattice-fringe image of berthierine-dominant, mixed-layer chlorite/berthierine in a composite chlorite-berthierine grain in sample KC-813. Terminations of chlorite layers (wide fringes) by berthierine (narrow fringes) are abundant, with three principal types schematically shown in the inset (see text for description).

several successive layers forming interface boundaries subparallel to (001).

Figure 7a shows a complex intergrowth of chlorite, berthierine, and mixed-layer chlorite/berthierine. Mineral boundaries are parallel or subparallel to (001). Kink bands, layer bending, and/or lens-shaped pores commonly are associated with the boundaries oblique to (001). The distribution of strain features is heterogeneous but lacks correlation with a specific phase except for the preferential occurrence of spots with high strain contrast in mixed-layer regions (lower middle and left of Figure 7b). The high-strain zones occurring between different phases are similar to the high-strain zone in chlorite described above.

Figure 7b shows a magnified portion of Figure 7a that illustrates typical random mixed-layer chlorite/berthierine and the textures at an interface boundary. The boundary on the right separates packets of berthierine and mixed-layer chlorite/berthierine. It consists of several kink bands that obscure the exact position of the interface in each layer. The electron diffraction patterns (Figure 7a) confirm the identifications of berthierine, mixed-layer chlorite/berthierine, and chlorite. The material on the left side of the high-strain boundary consists of parallel packets of chlorite, mixed-layer chlorite/berthierine, and berthierine, with two areas having high strain contrast. Similar strain features are also present in the interstratified chlorite/berthierine region of Figure 6, but not in highly strained chlorite crystals (Figure 5). Such strain features may be a result of accumulation of lateral misfits of layers due to differences in composition of octahedral sheets. Because the compositions of the brucite-like sheet and the octahedral sheet of the 2:1 layer of chlorite are different and because no compositional variations were observed over the chlorite and berthierine layers, the composition and lateral dimension of the octahedral sheets in berthierine layers must be different from those of chlorite. This in turn results in different tetrahedral sheet compositions and distortions in berthierine and chlorite layers. Lattice strain consequently may occur if there is a coherent or semicoherent relation between adjacent berthierine and chlorite layers. Strain contrast due to such lattice misfit has been demonstrated at a muscovite-biotite interface by Iijima and Zhu (1982).

Figure 8 shows some features in a sea of berthierine layers that are uncharacteristic of prograde mixed-layer chlorite/berthierine. The whole berthierine-dominant region is directly adjacent to a packet of parallel, pure chlorite layers (middle left of Figure 7a). Single layers or very thin packets of chlorite layers that are isolated or extend from the adjacent chlorite crystals are interstratified with thick packets of berthierine. Termina-

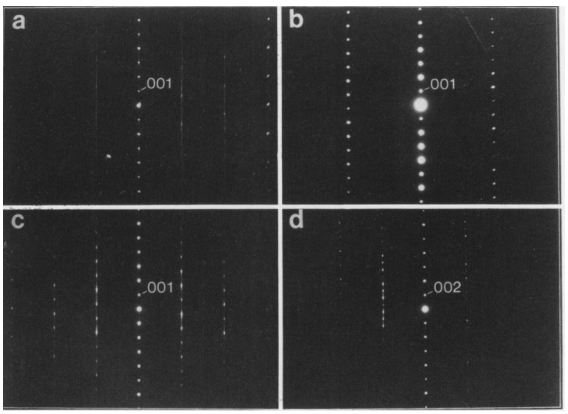

Figure 9. Electron diffraction patterns of (a) [110] (or [100]) zone of a one-layer polytype of chlorite with semi-random stacking (sample KC-813), (b) [010] zone of a regular one-layer polytype of chlorite with $\beta \cong 97°$ (sample KC-2505), (c) [100] zone of a regular one-layer polytype of triclinic chlorite with $\alpha \cong 102°$ (sample KC-813), and (d) [100] zone of a two-layer polytype of chlorite (sample KC-813).

tion of a chlorite fringe against two 7-Å fringes of berthierine commonly occurs with the chlorite layer imaged as one dark and one light grey fringe, corresponding to talc-like and brucite-like layers, or vice versa, depending upon focus conditions and crystal thickness and orientation (lower middle and A in the inset of Figure 8; Guthrie and Veblen, 1990). All of these features have not been observed previously in mixed-layer chlorite/berthierine in prograde diagenetic/metamorphic rocks (e.g., Lee and Peacor, 1983; Ahn and Peacor, 1985; Amouric *et al.*, 1988; Jahren and Aagaard, 1989; Hughes, 1989).

In the middle left of Figure 8 (also schematically illustrated in C of the inset), three chlorite layers convert to two chlorite plus two berthierine layers from right to left, with the two layers of berthierine positioned above and below the two chlorite layers. It appears that an upward displacement of the two chlorite layers on the left by ~7 Å occurred before formation of the surrounding berthierine layers, because no distortion of other layers is observed in the area. It is likely that such an interface was a dislocation in an original chlorite crystal prior to the formation of berthierine, as in the texture shown in Figure 4. A similar texture is present in the upper-left corner of Figure 8, but with apparent transitions of a talc-like layer and a brucite-like sheet (comprising a chlorite layer) to a brucite-like sheet and a talc-like layer, respectively (schematically depicted in B of the inset). Such textures are inferred to represent true transition features because there are no obvious strain contrast or abrupt changes of crystal orientation and thickness, and because through-focus imaging confirms the existence of structural changes, albeit with a lack of one-to-one fringe-structure correspondence.

Polytypism

Precise determination of polytypes is difficult because many factors other than stacking sequence may affect the relative intensities of reflections in electron diffraction patterns. However, as shown below, some basic identification of chlorite and berthierine polytypism can be obtained without considering detailed stacking sequences and relative intensities of reflections. This section demonstrates the heterogeneity of chlorite polytypism and coherency relations between interstratified chlorite and berthierine in the Kidd Creek samples.

Figure 9 shows typical electron diffraction patterns of chlorite. In Figure 9a, chlorite exhibits continuous streaking along c* in 11*l* and 22*l* (or 02*l* and 04*l*) reflection rows but not in 00*l* and 33*l* (or 06*l*) reflection rows. This pattern indicates a one-layer polytype of chlorite with semi-random stacking having adjacent layers related by $\pm b/3$ shifts along three pseudohexagonal *Y* axes (Bailey, 1988b). Figure 9b shows a pattern with the electron beam parallel to [010] of chlorite. The pattern indicates that the chlorite has $\beta \cong 97°$. Such a pattern commonly is associated with a [100] zone pattern characteristic of a one-layer polytype with semi-random stacking (Figure 9a) or of a regular one-layer polytype with $\alpha = 90°$ (Figure 3), most likely a II*b* polytype (Brown and Bailey, 1962). Figure 9c is a pattern of the [l00] zone of chlorite displaying well-defined 0*kl* reflections with 14-Å periodicity. It is a regular one-layer polytype of chlorite with $\alpha \cong 102°$, consistent with a I*b*-3 or II*ab*-4 polytype (Bailey, 1988b). Weak streaks parallel to c* in 02*l* and 04*l* reflection rows imply the presence of stacking faults. Figure 9d shows a diffraction pattern of a two-layer polytype of chlorite. The presence of ~28-Å periodicity in $k \neq 3n$ but not in $k = 3n$ 0*kl* reflection rows suggests that the two-layer periodicity is not due to a regular alternation of octahedral cations between I and II sites in the talc-like layers and/or brucite-like sheets of adjacent 14-Å chlorite layers, as observed by Lister and Bailey (1967), for example. Regular alternation of stacking relations between talc-like layers and interlayer brucite-like sheets with only one basic type of chlorite 14-Å layer is the probable explanation for this two-layer polytype of chlorite. Figure 9d also shows weak streaks along c* in $k \neq 3n$ reflection rows, implying local semi-random stacking, probably owing to the presence of stacking faults formed during deformation. A one-layer polytype with semi-random stacking is the dominant polytype in both samples KC-813 and KC-2505. No differences in composition were observed among the different polytypes of chlorite.

Berthierine invariably displays 7-Å periodicity in $k = 3n$ reflection rows and intense streaking along c* in $k \neq 3n$ reflection rows (Figure 10a), implying a semi-random stacking sequence similar to that in the one-

layer polytype of chlorite (Figure 9a). Figure 10b shows a typical electron diffraction pattern of the Kidd Creek mixed-layer chlorite/berthierine. The pattern shows only one set of non-00*l* reflections and streaks along c* in $k \neq 3n$ reflection rows that are much stronger than those due to mixed layering in $k = 3n$ reflection rows. Such a pattern implies that the berthierine and chlorite layers in the mixed-layer chlorite/berthierine are probably related by ±120° rotations about *c*. Coherent or semi-coherent relations between chlorite and berthierine layers are therefore inferred to occur in the mixed-layer chlorite/berthierine. The latter is more likely, judging from the observation of areas with significant strain contrast due to lattice misfit. These relations imply that at least some growth occurred by epitaxial overgrowth or replacement.

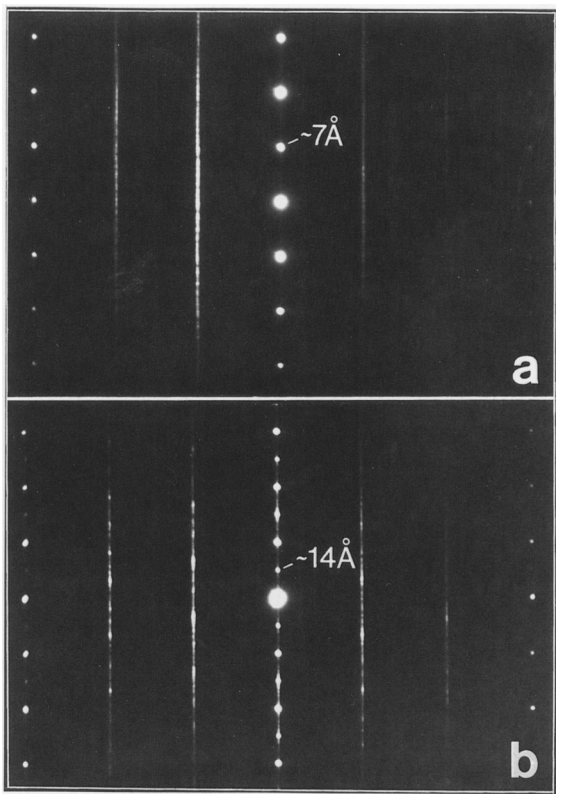

Figure 10. Electron diffraction patterns of (a) berthierine and (b) mixed-layer chlorite/berthierine. Streaks along c* in $k \neq 3n$ reflection rows suggest a semi-random stacking sequence in berthierine. Pattern (b) has only one set of non-00*l* reflection rows that shows much stronger streaks in $k \neq 3n$ than in $k = 3n$ reflection rows, implying a semi-random stacking relation in the mixed-layer sequence.

Chemical analyses

Table 1 shows representative compositions determined by AEM (total of 70 analyses) of berthierine, mixed-layer chlorite/berthierine, and chlorite in samples KC-2505 and KC-813. Analyses were obtained only from areas that had been characterized by lattice-fringe images and electron diffraction patterns.

Different schemes for the normalization of chlorite analyses give rise to very different formulae for octahedral sites. For example, normalization is often based on charge balance relative to an ideal number of anions. Such a method commonly requires octahedral vacancies if the number of total octahedral trivalent cations exceeds the number of tetrahedral trivalent cations. However, data from refined chlorite structures do not support the occurrence of such vacancies. Incorporation of siliceous phases into chlorite could result in apparent octahedral vacancies in a chlorite formula, as suggested by Bailey (1988c), whereas interlayering of other phyllosilicates such as smectite or talc commonly give the same results (e.g., Shau *et al.*, 1990). In our experience, however, trioctahedral chlorite samples that have been well characterized by TEM and proven to be pure phases invariably display charge balance and full octahedral occupancy, within analytical error (e.g., Shau *et al.*, 1990). Normalization of formulae based on charge balance that results in octahedral vacancies in pure trioctahedral chlorite, therefore, is not based

Table 1. Representative analytical electron microscope analysis of berthierine, chlorite, and mixed-layer chlorite/berthierine in samples KC-2505 and KC-813 from the Kidd Creek massive sulfide deposit.[1,2]

	KC-2505									KC-813				
	C_{Mg}	C_{Mg}	C_{Fe}	C_{Fe}	C/B	C/B	C/B	Ber	Ber	C_{Fe}	C_{Fe}	C/B	Ber	Ber
Si	4.90	5.10	4.98	4.99	4.82	5.15	5.21	4.71	4.97	4.95	5.00	5.13	5.03	5.01
Al	5.94	6.00	5.90	5.93	6.33	5.89	5.77	5.76	6.01	6.00	6.00	6.04	5.82	6.12
Fe^{3+}	0.26	0	0.14	0.09	0.01	0	0	0.82	0.05	0.10	0	0	0.10	0
Fe^{2+}	6.38	6.52	7.17	8.43	7.47	8.06	7.56	7.89	8.39	8.23	8.51	8.57	8.71	8.52
Mg	2.44	2.31	1.74	0.55	1.27	0.87	1.37	0.71	0.54	0.57	0.35	0.11	0.17	0.19
Mn	0.08	0.07	0.08	0.01	0.11	0.03	0.09	0.11	0.04	0.15	0.14	0.15	0.18	0.16
[ ][3]	0	0.07	0	0	0	0.07	0.07	0	0	0	0	0.11	0	0.05

[1] Normalization is based on 20 tetrahedral and octahedral cations total. Fe^{3+} is determined for charge balance with 20O + 16OH. Two standard deviations = ~0.10–0.15 for Si, Al, Fe, and Mg, based on counting statistics. Ti, Na, K, and Ca < 0.01 per formula unit.

[2] C_{Mg} = Fe-Mg chlorite, C_{Fe} = Fe-rich chlorite, C/B = mixed-layer chlorite/berthierine, Ber = berthierine.

[3] [ ] = octahedral vacancies with normalization on the basis of $O_{20}(OH)_{16}$.

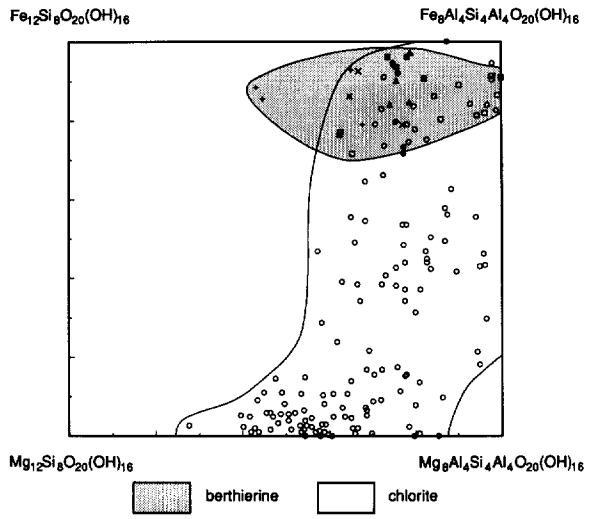

Figure 11. Compositional fields of berthierine and chlorite in a $Fe_{12}Si_8O_{20}(OH)_{16}$-$Mg_{12}Si_8O_{20}$-$(OH)_{16}$-$Fe_8Al_4Si_4Al_4$-$O_{20}(OH)_{16}$-$Mg_8Al_4Si_4Al_4O_{20}(OH)_{16}$ quaternary diagram. ○ = chlorite from Foster (1962), □ = berthierine from Bhattacharyya (1983), + = berthierine from Hughes (1989), × = chlorite from Hughes (1989), ● = chlorite from this study, ■ = berthierine from this study, ▲ = mixed-layer chlorite/berthierine from this study. All data are normalized on the basis of 20 total tetrahedral and octahedral cations. Minor Mn contents are included with Mg contents, and minor alkali and Ca contents are excluded in the normalization.

on verified structure relations. Such normalization adds an additional variable that complicates the interpretation of chlorite compositions. The same problem is even more acute in normalization of berthierine analyses for samples from other localities because of the lack of pure crystals with sizes large enough for electron microprobe analyses. In this study formulae of chlorite and berthierine are normalized on the basis of a total of 20 tetrahedral and octahedral cations. The relative numbers of Fe^{2+} and Fe^{3+} ions are then determined by charge balance, with the assumption that there are no vacancies in the octahedral sheets.

AEM analyses suggest that the Al and Si contents of chlorite and berthierine in samples KC-2505 and KC-813 do not vary significantly. The numbers of Al and Si atoms are nearly equal to 6 and 5, respectively, consistent with previous electron microprobe analyses (Slack and Coad, 1989; Slack *et al.*, 1992). The chlorite in sample KC-2505 is divided into two groups on the basis of composition; both are relatively iron rich, but one is more so than the other. The latter (Fe-Mg chlorite) is relatively homogeneous (Fe/(Fe+Mg) ≅ 0.70–0.75) and, along with muscovite, is the dominant phyllosilicate in sample KC-2505. The subordinate Fe-rich chlorite has a variable composition (Fe/(Fe+Mg) ≅ 0.80–0.95). Most of the berthierine has Si and Al contents similar to those of chlorite but has higher Fe contents (Fe/(Fe+Mg) ≥ 0.90) than most of the chlorite. Mixed-layer chlorite/berthierine shows a range of Fe/Mg ratios and a slightly larger variation in Al/Si ratios. Relatively Fe-rich, mixed-layer chlorite/berthierine commonly is associated with the Fe-rich chlorite.

Chlorite in sample KC-813 is compositionally homogeneous despite polytypic and textural variations, and is as Fe-rich as the coexisting berthierine. The composition of mixed-layer chlorite/berthierine in the sample is not significantly different from those of the chlorite and berthierine. The chlorite (Fe/(Fe+Mg) = 0.90–0.97) and mixed-layer chlorite/berthierine (Fe/(Fe+Mg) = 0.95–0.99) are much more Fe-rich than their equivalents in sample KC-2505. In both samples, berthierine generally has Al and Si contents identical to those of chlorite, but slightly lower Si contents were also detected in some berthierine. All of these phases have minor amounts of Mn.

DISCUSSION

Can berthierine be a polymorph of Fe-rich chlorite?

Syntheses of chlorite commonly yield 7-Å and/or 14-Å phases that are considered to have a polymorphic relation because they were synthesized under the same bulk chemical conditions and/or are inferred (based on X-ray powder diffraction) to have similar compositions (e.g., Nelson and Roy, 1958; Velde, 1973; James *et al.*, 1976). For natural systems, the term "polymorph" has often been used for clay minerals that are known to be related by stacking differences, but for which chemical identity is unproven. The most obvious example is $1M_d$ and $2M_1$ illite, which may have different compositional ranges that have not been well defined. In the same sense, berthierine or poorly-defined 7-Å phases in low grade rocks are commonly viewed as a precursor polymorph of chlorite, analogous to the dioctahedral mica sequence (Velde *et al.*, 1974; Iijima and Matsumoto, 1982; Lee and Peacor, 1983; Ahn and Peacor, 1985; Curtis *et al.*, 1985; Jahren and Aagaard, 1989). However, in a strict sense, polymorphs must have identical compositions. Overlapping of compositional fields of chlorite and berthierine has been noted by Curtis *et al.* (1985), Hughes (1989), Jahren and Aagaard (1989), and Velde (1989), but emphasis has focused on chemical comparisons rather than on polymorphic relations. This, in part, is because most available analyses of berthierine have been obtained by electron microprobe on rock samples or clay separates, for which contamination by other phases is likely. Also, such a polymorphic relation customarily has been assumed to exist. However, we are unaware of the existence of any accurate analyses of 7- and 14-Å phases that have been proven by TEM observation to be pure and that have demonstrated polymorphism.

Compositions of the Kidd Creek berthierine and chlorite and those reported in Foster (1962), Bhatta-

charyya (1983), and Hughes (1989) are plotted on the $Fe_{12}Si_8O_{20}(OH)_{16}$-$Mg_{12}Si_8O_{20}(OH)_{16}$-$Mg_8Al_4Si_4Al_4O_{20}(OH)_{16}$-$Fe_8Al_4Si_4Al_4O_{20}(OH)_{16}$ quaternary diagram in Figure 11. The diagram covers four principal end members, involving (Mg,Fe)-Al and Al-Si substitutions in chlorite. All other trivalent and quadrivalent cations except Si are treated as substitutions for Al. Because most chlorite and berthierine only have minor amounts of tri- or quadrivalent cations that may act like Al, such a treatment is reasonable for the purposes of this comparison. Even though most berthierine is relatively Al- and Fe-rich compared with chlorite (most are metamorphic chlorites from Foster, 1962), there is a limited range of compositions for which there is true polymorphism (Figure 11). Mn and Fe^{3+} have been shown to occur in berthierine as well as in chlorite of similar compositions, but such substitutions occur for ions of similar radius at the minor-to-trace level in both phases; therefore they have negligible effects on polymorphic relations.

Brindley (1982) suggested that octahedral vacancies may exist in berthierine. If vacancies do indeed occur in berthierine but not in associated chlorite, it is possible that normalization of berthierine formulae on an incorrect basis might imply a fictitious similarity in composition between berthierine and chlorite, and therefore in polymorphism. As noted above, such vacancies are generally assumed to exist if normalization is based on charge balance relative to an ideal number of anions, resulting in an excess of octahedral trivalent cations relative to tetrahedral trivalent cations, as is common for chlorite (e.g., Curtis *et al.*, 1985; Hillier and Velde, 1991). There is no apparent chemical discrimination between berthierine and Fe-rich chlorite in terms of the number of octahedral vacancies if they both are normalized in the same manner. Berthierine typically is very fine-grained, especially in low-grade sediments. Even microprobe analyses are likely to suffer from contamination, as is commonly the case for chlorite (Bailey, 1988c). Indeed, the Kidd Creek berthierine described here is very coarse-grained, relative to other berthierine occurrences, but most of the electron microprobe analyses (Slack and Coad, 1989; Slack *et al.*, 1992) were subject to contamination even for these specimens. However, AEM analyses were obtained in this study only for berthierine that had been well-characterized by TEM. The resulting analyses (Table 1) are consistent with a lack of vacancies, or with a small number of vacancies within analytical error, even if normalized to anions, $O_{20}(OH)_{16}$. Therefore, the overlap in composition of Fe-chlorite and berthierine indicates a polymorphic relation for a limited range of Fe, Al-rich compositions. Such polymorphs may coexist under conditions of stable equilibrium only under the very unlikely and specific P-T conditions corresponding to univariant equilibrium. Although such a possibility cannot be entirely disregarded, it is highly probable that either the berthierine or Fe-chlorite having compositions in the region of overlap were metastable under the conditions of formation at Kidd Creek. This conclusion is consistent with other relations, as described below.

Alteration of chlorite to berthierine

The presence of chlorite of two distinctly different compositions and the lack of chemical homogeneity of each type of chlorite in sample KC-2505 is definitive evidence that the assemblage is not in a state of stable equilibrium. The presence of berthierine and four different polytypes of chlorite having the same compositions is also indicative of non-equilibrium conditions.

Chlorite and berthierine are interstratified in a wide range of complex relations, from mixed layering of small numbers (<5) of layers to interstratification of thick packets of layers and high concentrations of layer terminations. Such relations are consistent with an intermediate stage of alteration from one phase to the other under non-equilibrium conditions, and imply a replacement mechanism for the origin of either berthierine or chlorite.

Berthierine has been inferred to occur as a metastable prograde precursor to chlorite in rocks undergoing diagenesis (Velde *et al.*, 1974; Iijima and Matsumoto, 1982; Jahren and Aagaard, 1989; Walker and Thompson, 1990). A small increase in diagenetic grade (or burial depth) results in replacement of berthierine by chlorite. The Kidd Creek area has experienced regional polymetamorphism to greenschist facies conditions together with multiple deformational events (Walker *et al.*, 1975; Nunes and Pyke, 1981; Percival and Krogh, 1983; Brisbin *et al.*, 1990; Barrie and Davis, 1990). Observations of deformational features and metamorphic reaction rims in tourmaline by Slack and Coad (1989) are consistent with pervasive metamorphic processes in the deposit. Under such conditions, preservation of pre-metamorphic berthierine and mixed-layer chlorite/berthierine in the Kidd Creek rocks is considered unlikely. Most of the Kidd Creek berthierine is likely to be a syn- to post-metamorphic hydrothermal or retrograde alteration product of chlorite.

In clastic sedimentary rocks, phyllosilicate stacks consisting of interstratified parallel or subparallel packets of two different phyllosilicate phases have been shown to originate from detrital phyllosilicate grains, with or without recrystallization, in response to diagenetic/metamorphic conditions (e.g., Roy, 1978; Craig *et al.*, 1982; van der Pluijm and Kaars-Sijpesteijn, 1984; Gregg, 1985; Woodland, 1985; Dimberline, 1986; Morad, 1986). Deformation features due to tectonic stress are commonly observed in such stacks. In the Kidd Creek rocks, Fe-Mg chlorite that is much more abundant than coexisting Fe-rich chlorite, berthierine, and mixed-layer chlorite/berthierine is commonly de-

formed. In sample KC-2505, Fe-Mg chlorite has a rather homogeneous composition, but with abundant strain features that were most likely generated by dynamic metamorphic events. This Fe-Mg chlorite is inferred to be a primary hydrothermal, pre-metamorphic product that originated during ore-forming processes, or a metamorphic phase that evolved from possible hydrothermal precursors such as smectite and mixed-layer chlorite/smectite. The presence of hybrid phases usually is suggested to result from retrograde metamorphic or hydrothermal reactions under non-equilibrium conditions (e.g., Banfield *et al.*, 1989; Jiang and Peacor, 1991). The complex, heterogeneous mixed-layer chlorite/berthierine, berthierine, and Fe-rich chlorite in sample KC-2505 have properties that are consistent with non-equilibrium states and, therefore, are likely alteration products of homogeneous Fe-Mg chlorite formed earlier. The deformation textures observed in berthierine and mixed-layer chlorite/berthierine, for example, could not have been inherited from a precursor, would have been annealed during metamorphism, and must have been caused by deformation subsequent to the replacement event.

The chlorite, berthierine, and mixed-layer chlorite/berthierine in sample KC-813 show a wide range of complex textural and structural relations but have similar compositions. The great variety of interstratifications and the styles of mixed layering are uncharacteristic of berthierine or mixed-layer chlorite/berthierine observed in prograde diagenetic/metamorphic rocks (Lee and Peacor, 1983; Ahn and Peacor, 1985; Amouric *et al.*, 1988; Jahren and Aagaard, 1989). Low-temperature, hydrothermal or retrograde alteration of one phyllosilicate to another commonly results in a wide range of intergrowth relations reflecting heterogeneous local environments (e.g., Veblen and Ferry, 1983; Yau *et al.*, 1984; Ahn and Peacor, 1987; Banfield and Eggleton, 1988; Jiang *et al.*, 1990; Sharp *et al.*, 1990; Jiang and Peacor, 1991). All of the phyllosilicate grains in sample KC-813 have high concentrations of strain features, such as kink bands and stacking faults, which apparently reflect the effect of tectonic stress during dynamic metamorphism. In addition, the presence of high-strain zones that transect the cleavage of phyllosilicate grains also suggests that at least one of the deformational events occurred after the formation of unaltered phyllosilicates. The separation of packets of berthierine, chlorite, and mixed-layer chlorite/berthierine of different structures and/or textures by high-strain zones implies that at least part of the replacement reaction took place after a deformational event, presumably after the peak of metamorphism. High-strain zones are also observed in chlorite grains that lack berthierine. Accordingly, it is highly probable that composite chlorite-berthierine grains in sample KC-813 originated from precursor grains of deformed chlorite. Such grains were altered to and replaced by the assemblage described above, but retain most of their original relations with other phases.

The Fe/(Fe+Mg) ratios of the Kidd Creek chlorite increase from the periphery of the deposit to the core of the footwall alteration zone, in areas containing massive rhyolite sills (Slack and Coad, 1989). It is possible that the Kidd Creek Fe-rich chlorite formed by pre-metamorphic hydrothermal alteration of primary hydrothermal Fe-Mg chlorite, in which the Fe-rich fluid originated during emplacement of the rhyolite sills (Slack and Coad, 1989). That interpretation is strengthened by the observations of this paper, but the Fe-Mg chlorite need not have formed prior to metamorphism and the replacement may have occurred during the polymetamorphic events described above. We have shown in this study that the Fe-rich chlorite was deformed during metamorphism, giving rise to abundant strain features that are consistent with either process. The Fe-rich chlorite in sample KC-2505 may have formed through similar processes, but with a greater degree of preservation of Fe-Mg chlorite. Both the Fe-rich and Fe-Mg chlorite in sample KC-2505 subsequently were partially altered to berthierine and/or mixed-layer chlorite/berthierine. The greater range of Fe-Mg compositions of berthierine and mixed-layer chlorite/berthierine in sample KC-2505, relative to sample KC-813, is consistent with such a process.

Berthierine and chlorite in other Kidd Creek samples may have originated by the same processes that affected samples KC-2505 and KC-813. However, textural evidence suggests a pre-metamorphic hydrothermal origin of berthierine in other samples from the deposit, as reported by Slack *et al.* (1992). For example, large euhedral berthierine grains (100–200 μm) are observed to coexist with apparent hydrothermal halloysite in some undeformed, pristine samples. It is possible that Fe-rich chlorite is unstable relative to berthierine under certain conditions, and that berthierine may have formed as an early hydrothermal phase or as a metamorphic mineral that persisted locally during the metamorphic events. Although the studied samples were chosen to be representative of the principal mineralogical relations, they are exceedingly small sources of data. It nevertheless is clear that much of the berthierine formed during or subsequent to polymetamorphic events, with some berthierine being pre-metamorphic in origin. Further work is necessary on additional samples in order to determine the full range of phyllosilicate origins in relation to the complex geologic history of the Kidd Creek area.

Geologic implications

Slack and Coad (1989) showed a general trend of increasing Fe/(Fe+Mg) ratios of chlorite from the periphery to the core of the footwall alteration zone in the Kidd Creek deposit. They also noted the wide variation in Fe and Mg contents of "chlorite" in some of

the samples (e.g., KC-2505) from the core of the alteration zone, and suggested that this pattern reflects mixing of primary Fe-rich end member hydrothermal fluids (generated during emplacement of the massive rhyolite sills) and Mg-rich seawater. The presence of wide variations in chlorite compositions within a few individual samples is inferred to be the result of retrograde or syn- or post-metamorphic alteration of primary chlorite. Differences in composition and texture of the berthierine are likely due to different compositions of primary (precursor) chlorite and to different styles and degrees of deformation among different samples. Such relations are consistent with the fluid mixing model of Slack and Coad (1989) and the heterogeneous nature of deformation in the mine area (Walker *et al.*, 1975; Brisbin *et al.*, 1990; Barrie and Davis, 1990).

Whereas berthierine is generally considered to be a prograde precursor to chlorite, the post-ore origin of berthierine admixed with hydrothermal or metamorphic chlorite at Kidd Creek implies that chlorite-berthierine assemblages of hydrothermal origin must be interpreted with caution. The results of this study also imply that berthierine can form as a replacement of chlorite; such replacement need not occur only in complex hydrothermal/metamorphic settings, however, but also may be characteristic of berthierine in iron formations or clastic sedimentary rocks.

ACKNOWLEDGMENTS

We are grateful to S. P. Altaner, R. E. Ferrell, Jr., G. L. Nord, Jr., M. Ross, and B. Velde for their critical reviews. This work was supported by NSF grants EAR-88-17080 and EAR-91-04565 to D. R. Peacor. The scanning transmission electron microscope used in this work was acquired under grant EAR-87-08276 from the National Science Foundation. We thank the staff and management of Kidd Creek Mines and Falconbridge Limited for providing drill core for study.

REFERENCES

Ahn, J. H. and Peacor, D. R. (1985) Transmission electron microscopic study of diagenetic chlorite in Gulf Coast argillaceous sediments: *Clays & Clay Minerals* **33,** 228–236.

Ahn, J. H. and Peacor, D. R. (1987) Kaolinization of biotite: TEM data and implications for an alteration mechanism: *Amer. Mineral.* **72,** 353–356.

Amouric, M., Gianetto, I., and Proust, D. (1988) 7, 10, and 14 Å mixed-layer phyllosilicates studied structurally by TEM in pelitic rocks of the Piemontese zone (Venezuela): *Bull. Mineral.* **111,** 29–37.

Bailey, S. W. (1984) Structure of layer silicates: in *Crystal Structures of Clay Minerals and Their X-Ray Identification,* G. W. Brindley and G. Brown, eds., The Mineralogical Society, London, 1–124.

Bailey, S. W. (1988a) Structures and compositions of other trioctahedral 1:1 phyllosilicates: in *Hydrous Phyllosilicates (Exclusive of Micas),* S. W. Bailey, ed., Mineralogical Society of America, Reviews in Mineralogy **19,** Washington, D.C., 169–188.

Bailey, S. W. (1988b) X-ray diffraction identification of the polytypes of mica, serpentine, and chlorite: *Clays & Clay Minerals* **36,** 193–213.

Bailey, S. W. (1988c) Chlorites: Structures and crystal chemistry: in *Hydrous Phyllosilicates (Exclusive of Micas),* S. W. Bailey, ed., Mineralogical Society of America, Reviews in Mineralogy **19,** Washington, D.C., 347–403.

Banfield, J. F. and Eggleton, R. A. (1988) Transmission electron microscope study of biotite weathering: *Clays & Clay Minerals* **36,** 47–60.

Banfield, J. F., Karabinos, P., and Veblen, D. R. (1989) Transmission electron microscopy of chloritoid: Intergrowth with sheet silicates and reactions in metapelites: *Amer. Mineral.* **74,** 549–564.

Barrie, C. T. and Davis, D. W. (1990) Timing of magmatism and deformation in the Kamiskotia-Kidd Creek area, western Abitibi subprovince, Canada: *Precam. Research* **46,** 217–240.

Bhattacharyya, D. P. (1983) Origin of berthierine in ironstones: *Clays & Clay Minerals* **31,** 173–182.

Bons, A.-J. (1988) Deformation of chlorite in naturally deformed low-grade rocks: *Tectonophysics* **154,** 149–165.

Brindley, G. W. (1982) Chemical compositions of berthierines—A review: *Clays & Clay Minerals* **30,** 153–155.

Brisbin, D., Kelly, V., and Cook, R. (1990) Kidd Creek mine: in *Geology and Ore Deposits of the Timmins District, Ontario,* J. A. Fyon and A. H. Green, eds., Eighth IAGOD Symposium, Field Trip Guidebook 6, Geol. Survey Canada Open File **2161,** 66–76.

Brown, B. E. and Bailey, S. W. (1962) Chlorite polytypism: I. Regular and semi-random one-layer structures: *Amer. Mineral.* **47,** 819–850.

Chamley, H. (1990) *Clay Sedimentology:* Springer-Verlag, New York, 623 pp.

Coad, P. R. (1985) Rhyolite geology at Kidd Creek—A progress report: *Can. Inst. Mining Metall. Bull.* **78,** 70–83.

Craig, J., Fitches, W. R., and Maltman, A. J. (1982) Chlorite-mica stacks in low-strain rocks from central Wales: *Geol. Magazine* **119,** 243–256.

Curtis, C. D., Hughes, C. R., Whiteman, J. A., and Whittle, C. K. (1985) Compositional variations within some sedimentary chlorites and some comments on their origin: *Mineral. Mag.* **49,** 375–386.

Dimberline, A. (1986) Electron microscope and microprobe analysis of chlorite-mica stacks in the Wenlock turbidites, mid Wales, U.K.: *Geol. Magazine* **123,** 299–306.

Edington, J. W. (1975) *Interpretation of Transmission Electron Micrographs, Monographs in Practical Electron Microscopy in Material Science, Vol. 3:* The MacMillan Press Ltd., London, 112 pp.

Ferrow, E. A., London, D., Goodman, K. S., and Veblen, D. R. (1990) Sheet silicates of the Lawler Peak granite, Arizona: Chemistry, structural variations, and exsolution: *Contrib. Mineral. Petr.* **105,** 491–501.

Foster, M. D. (1962) Interpretation of the composition and a classification of the chlorites: *U.S. Geol. Survey Prof. Paper* **414A,** A1–A33.

Frey, M. (1970) The step from diagenesis to metamorphism in pelitic rocks during Alpine orogenesis: *Sedimentology* **15,** 261–279.

Frey, M. (1978) Progressive low-grade metamorphism of a black shale formation, central Swiss Alps, with special reference to pyrophyllite and margarite bearing assemblages: *J. Petrol.* **19,** 95–135.

Goodwin, L. B. and Wenk, H.-R. (1990) Intracrystalline folding and cataclasis in biotite of the Santa Rosa mylonite zone: HVEM and TEM observations: *Tectonophysics* **172,** 201–214.

Gregg, W. J. (1985) Deformation of chlorite-mica aggregates

in cleaved psammitic and pelitic rocks from Islesboro, Maine, U.S.A.: *J. Struc. Geol.* **8,** 59–68.

Guthrie, G. D., Jr. and Veblen, D. R. (1990) Interpreting one-dimensional high-resolution transmission electron micrographs of sheet silicates by computer simulation: *Amer. Mineral.* **75,** 276–288.

Hillier, S. and Velde, B. (1991) Octahedral occupancy and the chemical composition of diagenetic (low-temperature) chlorites: *Clay Miner.* **26,** 149–168.

Hughes, C. R. (1989) The application of analytical transmission electron microscopy to the study of oolitic ironstones: A preliminary study: in *Phanerozoic Ironstones,* T. P. Young and W. E. G. Taylor, eds., Geological Society Special Publication No. 46, The Geological Society, London, 121–131.

Iijima, A., and Matsumoto, R. (1982) Berthierine and chamosite in coal measures of Japan: *Clays & Clay Minerals* **30,** 264–274.

Iijima, S. and Zhu, J. (1982) Electron microscopy of a muscovite-biotite interface: *Amer. Mineral.* **67,** 1195–1205.

Jahren, J. S. and Aagaard, P. (1989) Compositional variations in diagenetic chlorites and illites, and relationships with formation-water chemistry: *Clay Miner.* **24,** 157–170.

James, R. S., Turnock, A. C., and Fawcett, J. J. (1976) The stability and phase relations of iron chlorite below 8.5 kb P_{H_2O}: *Contr. Mineral. Petr.* **56,** 1–25.

Jiang, W.-T. and Peacor, D. R. (1991) Transmission electron microscopic study of the kaolinitization of muscovite: *Clays & Clay Minerals* **39,** 1–13.

Jiang, W.-T., Peacor, D. R., Merriman, R. J., and Roberts, B. (1990) Transmission and analytical electron microscopic study of mixed-layer illite/smectite formed as an apparent replacement product of diagenetic illite: *Clays & Clay Minerals* **38,** 449–468.

Kisch, H. J. (1983) Mineralogy and petrology of burial diagenesis (burial metamorphism) and incipient metamorphism in clastic rocks: in *Diagenesis in Sediments and Sedimentary Rocks, 2,* G. Larsen and G. V. Chilingar, eds., Elsevier, New York, 289–493.

Lee, J. H. and Peacor, D. R. (1983) Interlayer transitions in phyllosilicates of Martinsburg shale: *Nature* **303,** 608–609.

Lister, J. S. and Bailey, S. W. (1967) Chlorite polytypism: IV. Regular two-layer structures: *Amer. Mineral.* **52,** 1614–1631.

Maas, R., McCulloch, M. T., Campbell, I. H., and Coad, P. R. (1986) Sm-Nd and Rb-Sr dating of an Archean massive sulfide deposit: Kidd Creek, Ontario: *Geology* **14,** 585–588.

Morad, S. (1986) Mica-chlorite intergrowths in very low-grade metamorphosed sedimentary rocks from Norway: *Neues Jahrbuch Mineral. Abh.* **154,** 271–287.

Nelson, B. W. and Roy, R. (1958) Synthesis of the chlorites and their structural and chemical constitution: *Amer. Mineral.* **43,** 707–725.

Nunes, P. D. and Pyke, D. R. (1981) Time-stratigraphic correlation of the Kidd Creek orebody with volcanic rocks south of Timmins, Ontario, as inferred from zircon U-Pb ages: *Econ. Geol.* **76,** 944–951.

Percival, J. A. and Krogh, T. E. (1983) U-Pb zircon geochronology of the Kapuskasing structural zone and vicinity in the Chapleau-Foleyet area, Ontario: *Can. J. Earth Sci.* **20,** 830–843.

Roy, A. B. (1978) Evolution of slaty cleavage in relation to diagenesis and metamorphism: A study from the Hunsrückschiefer: *Geol. Soc. Amer. Bull.* **89,** 1775–1785.

Sharp, T. G., Otten, M. T., and Buseck, P. R. (1990) Serpentinization of phlogopite phenocrysts from a micaceous kimberlite: *Cont. Mineral. Petr.* **104,** 530–539.

Shau, Y-H., Peacor, D. R., and Essene, E. J. (1990) Corrensite and mixed-layer chlorite/corrensite metabasalt from northern Taiwan: TEM/AEM, EPMA, XRD, and optical studies: *Cont. Mineral. Petr.* **105,** 123–142.

Slack, J. F. and Coad, P. R. (1989) Multiple hydrothermal and metamorphic events in the Kidd Creek volcanogenic massive sulphide deposit, Timmins, Ontario: Evidence from tourmalines and chlorites: *Can. J. Earth Sci.* **26,** 694–715.

Slack, J. F., Jiang, W.-T., Peacor, D. R., and Okita, P. M. (1992) Hydrothermal and metamorphic berthierine from the Kidd Creek volcanogenic massive sulfide deposit, Timmins, Ontario: *Can. Mineral.,* in press.

Taylor, K. G. (1990) Berthierine from the non-marine Wealdon (Early Cretaceous) sediments of south-east England: *Clay Miner.* **25,** 391–399.

van der Pluijm, B. A. and Kaars-Sijpesteijn, C. H. (1984) Chlorite-mica aggregates: Morphology, orientation, development and bearing on cleavage formation in very low-grade rocks: *J. Struct. Geol.* **6,** 399–407.

Veblen, D. R. (1983) Microstructures and mixed layering in intergrown wonesite, chlorite, talc, biotite, and kaolinite: *Amer. Mineral.* **68,** 566–580.

Veblen, D. R. and Ferry, J. M. (1983) A TEM study of the biotite-chlorite reaction and comparison with petrologic observations: *Am. Mineral.* **68,** 1160–1168.

Velde, B. (1973) Phase equilibria in the system MgO-Al_2O_3-SiO_2-H_2O: Chlorites and associated minerals: *Mineral. Mag.* **39,** 297–312.

Velde, B. (1985) *Clay Minerals: A Physico-Chemical Explanation of Their Occurrence:* Elsevier, Amsterdam, 427 pp.

Velde, B. (1989) Phyllosilicate formation in berthierine peloids and iron oolites: in *Phanerozoic Ironstones,* T. P. Young and W. E. G. Taylor, eds., The Geological Society, London, Spec. Publ. No. 46, 3–8.

Velde, B., Raoult, J. F., and Leikine, M. (1974) Metamorphosed berthierine pellets in Mid-Cretaceous rocks from northeastern Algeria: *J. Sediment. Petrol.* **44,** 1275–1280.

Walker, J. R. and Thompson, G. R. (1990) Structural variations in chlorite and illite in a diagenetic sequence from the Imperial Valley, California: *Clays & Clay Minerals* **38,** 315–321.

Walker, R. R., Matulich, A., Amos, A. C., Watkins, J. J., and Mannard, G. W. (1975) The geology of the Kidd Creek mine: *Econ. Geol.* **70,** 80–89.

Weaver, C. E. (1989) *Clays, Muds, and Shales:* Elsevier, Amsterdam, 819 pp.

Woodland, B. G. (1985) Relationship of concretions and chlorite-muscovite porphyroblasts to the development of dominant cleavage in low-grade metamorphic deformed rocks from north-central Wales, Great Britain: *J. Struc. Geol.* **7,** 205–215.

Worden, R. H., Droop, G. T. R., and Champness, P. E. (1991) The reaction antigorite → olivine + talc + H_2O in the Bergell aureole, N. Italy: *Mineral. Mag.* **55,** 367–377.

Yau, Y. C., Anovitz, L. M., Essene, E. J., and Peacor, D. R. (1984) Phlogopite-chlorite reaction mechanisms and physical conditions during retrograde reactions in the Marble Formation, Franklin, New Jersey: *Contr. Mineral. Petr.* **88,** 299–306.

Young, T. P. (1989) Phanerozoic ironstones: An introduction and review: in *Phanerozoic Ironstones,* T. P. Young and W. E. G. Taylor, eds., Geological Society Special Publication No. 46, The Geological Society, London, ix–xxv.

(Received 27 February 1992; accepted 7 August 1992; Ms. 2192)